International Journal of Gastroenterology
2023; 7(1): 1-14
http://www.sciencepublishinggroup.com/j/ijg
doi: 10.11648/j.ijg.20230701.11
ISSN: 2640-1681 (Print); ISSN: 2640-169X (Online)

The Homeostatic Protein Fam3D Orchestrates Colon Mucosal Protection Against Infection, Inflammation, and Carcinogenesis

Keqiang Chen[1, *], Weiwei Liang[1, 2], Teizo Yoshimura[1], Wanghua Gong[3], Jiaqiang Huang[1, 4], Simone Difilippantonio[5], Georgette Jones[5], Jimmy York[5], Giorgio Trinchieri[6], Ying Wang[7, *], Ji Ming Wang[1, *]

[1]Laboratory of Cancer Innovation, Center for Cancer Research, National Cancer Institute at Frederick, Frederick, USA

[2]Department of Gastroenterology, Guangzhou Institute of Pediatrics, Guanzhou Women and Children's Medical Center, Guangzhou Medical University, Guangzhou, China

[3]Basic Research Program, Leidos Biomedical Research, Inc., Frederick, USA

[4]College of Life Sciences, Beijing Jiaotong University, Beijing, China

[5]Gnotobiotics Facility, Frederick National Laboratory for Cancer Research, Frederick, USA

[6]Laboratory of Integrative Cancer Immunology, Center for Cancer Research, National Cancer Institute, Bethesda, USA

[7]Department of Immunology, School of Basic Medical Sciences and Key Laboratory of Medical Immunology, Peking University, Beijing, China

Email address:

chenkeq@mail.nih.gov (Keqiang Chen), yw@bjmu.edu.cn (Ying Wang), wangji@ mail.nih.gov (Ji Ming Wang)

[*]Corresponding author

To cite this article:

Keqiang Chen, Weiwei Liang, Teizo Yoshimura, Wanghua Gong, Jiaqiang Huang, Simone Difilippantonio, Georgette Jones, Jimmy York, Giorgio Trinchieri, Ying Wang, Ji Ming Wang. The Homeostatic Protein Fam3D Orchestrates Colon Mucosal Protection Against Infection, Inflammation, and Carcinogenesis. *International Journal of Gastroenterology*. Vol. 7, No. 1, 2023, pp. 1-14. doi: 10.11648/j.ijg.20230701.11

Received: January 19, 2023; **Accepted**: February 10, 2023; **Published**: February 21, 2023

Abstract: Fam3D (FAM3D in human) is a homeostatic protein expressed mainly in gastrointestinal tract that plays an essential role in promoting colon mucosal development and homeostasis. However, the mechanistic basis for the action of Fam3D, particularly its relationship to colon mucosal development and microbiome balance, is less clear. In this study, Fam3D expression was increased in colon epithelial cells of germ-free (GF) *Fam3D*$^{+/+}$ mice following *E. coli* infection and GF *Fam3D*$^{-/-}$ mice were more susceptible to *E. coli* colonization in the colon. In chemically induced colitis and colon cancer, GF *Fam3D*$^{-/-}$ mice showed more severe inflammatory responses, colon mucosal damage, and tumorigenesis. Unlike SPF mice, GF *Fam3D*$^{-/-}$ mice exhibited decreased production of the gut barrier protein Muc2. Mechanism study revealed that in colon epithelial cells, LPS upregulated Fam3D expression through TLR4, while Fam3D promoted Muc2 production through Fpr1 and Fpr2. In addition, Fam3D also upregulated the expression of MAP kinase phosphatase 1 (MKP-1) which is crucial for restraining inflammatory responses. Fam3D deficiency reduced MKP-1 expression, thereby increasing IL-1β and TNF-α production in colon mucosa of GF mice. Thus, Fam3D is critical in colon homeostasis and constitutes a therapeutic target for inflammatory colon diseases.

Keywords: Fam3D, Muc2, MKP-1, Infection, Inflammation, Colon Cancer

1. Introduction

Colorectal cancer (CRC) is considered to be one of the most common malignant tumors that endanger huma health [1, 2]. Accumulating evidence reveals that inflammation plays an important role on CRC development including tumor growth and angiogenesis. One of the major hallmarks in inflammation related with CRC is the upregulation of inflammatory cytokines which causes abnormal immune cell

function [3]. Although the exact mechanism that inflammation is associated with CRC remains unclear, anti-inflammatory therapeutics aided in impeding the development of CRC [4].

The mucous layer located on the surface of colon mucosa is an integral component of the non-immune portion of the gut barrier, in which MUC2 is key component of the mucous layer [5]. MUC2 mucin produced by epithelial goblet cells is a secretory protein, which prevents intestinal bacteria from contacting colonic epithelial cells and limits overall pathogen and commensal bacteria contact with the colonic mucosal surface [6, 7]. In acute intestinal infection by parasites, viruses, and bacteria, mucous secretion is rapidly increased to assist in the elimination of pathogens [8]. The mucus became thinner and discontinuous in the colon mucosa of the patients with ulcerative colitis (UC) and excrete less MUC2 mucin [9]. Patients with CRC showed reduced MUC2 production, which gradually decreases with the progression of the disease, resulting in the destruction of the epithelial barrier [10, 11]. Thus, MUC2 is crucial in maintaining the colon homeostasis. It is interesting that certain bacteria or their metabolites play an important role on the establishment of complete MUC2 mucus structure and function because germ-free (GF) mice display thin mucin layer and even absent locally. However, the mucus barrier of the colon can become thick and impenetrable in GF mice when colonized with complex microbial communities [12-15].

Extracellular signal-regulated kinase (ERK), Jun kinase (JNK/SAPK) and p38 MAPK belong to the family of mitogen-activated protein kinases (MAPKs) [16]. MAPKs are associated with transmitting extracellular signals to the nucleus leading to gene regulation and regulating the production of the pro-inflammatory cytokines and signaling events that lead to inflammation [17]. MAP kinase phosphatase 1 (MKP-1) is a founding member of the MKP family. MKP-1 is able to dephosphorylate all three members of the MAPK family [18] forming a negative feedback loop of MAPK activity with anti-inflammatory effects [19].

Family with sequence similarity 3, member D (FAM3D, Fam3D in mice) [20] was identified as a host-derived endogenous chemotactic agonist for the G-protein coupled chemoattractant receptors, formyl peptide receptor (FPR) 1 and FPR2 (mouse Fpr1 and Fpr2) [21, 22]. Recent studies in *Fam3D*$^{-/-}$ mice showed that Fam3D is crucial in maintaining the microbiota balance and protecting colon mucosa against inflammation and colon tumorigenesis [23]. Fam3D deficiency impaired the integrity of colonic mucosa and microbiota balance, promoted epithelial hyper-proliferation, reduced antimicrobial peptide production, and increased sensitivity to chemically induced colitis and the associated cancer [23]. The analysis of TCGA and CPTAC data showed that the levels of FAM3D mRNA and protein were significantly lower in human CRC tissues. FAM3D transcripts were expressed at lower levels in all stages of CRC and the protein was more poorly expressed in higher stages of CRCs [23], suggesting that FAM3D may act as an anti-cancer molecule in human CRC. However, the precise role of FAM3D in the colon homeostasis is unclear. In this study, by using GF mice, Fam3D was demonstrated to be a key player for the integrity of colon mucosa and the protection of the colon against infection, inflammation, and tumorigeneses.

2. Methods

2.1. Germ Free (GF) Mice

Pregnant donor females *Fam3D*$^{+/+}$ and *Fam3D*$^{-/-}$ mice were injected with progesterone (5 mg/ml) on gestational days 17.5 and 18.5. On gestational days 19.5, the donor female was euthanized, and the uterus submerged in a tube containing a warm Virkon solution and introduced into an isolator housing. The uterus was opened, and the pups were fostered by germ-free Swiss foster mothers. Weaned animals were tested and confirmed to be free of any viruses, bacteria, fungi, or parasites. GF mice were maintained in a sterile environment completely devoid of microorganisms in Gnotobiotic Facility, Frederick National Laboratory for Cancer Research, Frederick, MD. The GF mice used in the experiments were 2-3 months old, and male (Except male and female in the mouse model of AOM-DSS-induced colon cancer) and all experiments were performed under sterile conditions.

2.2. Cell Culture

CT26 mouse colon carcinoma cell line was maintained in Dulbecco's modified Eagle's medium (DMEM) (Gibco-Invitrogen) containing 10% FBS (HyClone Laboratories, Logan, UT, USA) and 1% penicillin/streptomycin. The CT26 cells were cultured in a humidified 37˚C incubator with 5% CO2.

2.3. Reagents

Recombinant mouse Fam3D was from Creative Biomart (Shirley, NY, USA). The purity of Fam3D > 90% as determined by SDS-PAGE and the endotoxin is < 1.0 eu per μg of the protein as determined by the LAL method. Rabbit polyclonal Fam3D antibody was from ThermoFisher (Waltham, MA USA). Anti-mouse Muc2, Ki67, MKP-1 and Goat anti *E. coli* antibodies were from Abcam (Boston, MA, USA). Anti-mouse IL-1β, TNF-α antibodies were from R&D Systems, Inc. (Minneapolis, MN, USA). Propidium Iodide (PI) was from Sigma-Aldrich (Rockville, MD, USA). Goat pAb to Rabbit IgG (Biotin), to Rat IgG (Biotin), to Mouse IgG were from Abcam. Donkey anti-goat IgG biotinylated antibody from R&D Systems, Inc (Minneapolis, MN, USA). PE Streptavidin and FITC Streptavidin were from Biolegend (San Diego, CA, USA). TLR4 inhibitor was from Sigma-Aldrich, WRW4 from Tocris (Minneapolis, MN, USA) and Boc-MLP and Cyclosporin H (CsH) were from R&D Systems, Inc.

2.4. Preparation of E. coli, Infection, and Measurement

E. coli was prepared as described [24]. *E. coli* O22:H8, which has been identified by whole genome sequencing and

stored in -80^{O}C, was thawed in a water bath with 37°C, and cultured in LB broth at 37°C, 180 rpm for 24 h, then determined for concentration basing on an OD600 nm of 0.4 corresponding to ~2×10^8 colony forming units (CFU)/ml. *E. coli* was washed three times with sterile phosphate-buffered saine (PBS) and discard the supernatant, then the pellets were diluted to 1×10^8 CFU/ml or 1×10^4 CFU/ml for future use.

For the infection with live E. coli, GF Fam3D$^{-/-}$ and Fam3D$^{+/+}$ mice were inoculated with 0.2 ml of the E. coli suspension containing 1×10^8 CFU/mouse by oral gavage. At day 5 post infection, Fam3D$^{-/-}$ and Fam3D$^{+/+}$ mice were sacrificed. The most distal 6 cm of the distal colon was harvested for OCT-embedded, frozen and section.

For measurement of *E. coli* number in Feces, fecal homogenates were diluted with sterile PBS into series of concentration and cultured in Violet Red Bile Lactose agar (VRBL, EMD Millipore Corporation), aerobically at 37^{O}C for 24 h and the number of bacterial colonies was counted. The results were represented as CFU/g feces (mean ± SD).

2.5. Mouse Models of Colitis and Colitis Associated Colon Cancer

For DSS induced colitis, GF mice were given 3% DSS (M. W. = 36,000-50,000, MP Biomedicals, LLC) in drinking water for 5 days followed by normal drinking water for 7 days to investigate mouse survival or 2 days to harvest colon samples for histopathological examination. For azoxymethane (AOM)-DSS induced colon cancer, GF mice were pre-inoculated with 0.2 ml of the *E. coli* suspension containing 1×10^4 CFU/mouse by oral gavage. 5 days later, mice were injected intraperitoneally with 10 mg/kg AOM (Sigma Aldrich). On day 6, mice were given 2% DSS in drinking water for 5 d, followed by 2 weeks of normal drinking water. DSS treatment was repeated for 3 cycles. Mouse death was defined by 20% body weight loss and/or other adverse clinical signs meeting the moribund criteria per ACUC guidelines.

2.6. Histology

OCT-embedded and frozen mouse distal colon sections with 10-μm-thickness were fixed in 10% neutral formalin solution for 20 min, washed with distilled H_2O for 2 min. These sections were stained with Hematoxylin/eosin (H&E) for analysis. The crypt damage score was defined as: 0. Intact crypt, 1. Loss of 1/3 of crypt, 2. Loss of 1/2 of crypt, 3. Loss of 2/3 of crypt, 4. Entire loss of crypt, 5. Loss of crypt and surface epithelia.

2.7. Immunofluorescence staining for Colon Sections and CT26 Epithelial Cells

Immunofluorescence analyses were performed on freshly frozen, OCT-embedded, and sectioned colon tissues (10-μm thick). For measurement of Fam3D, Muc2, Ki67, *E. coli*, MKP-1, IL-1β, TNF-α, sections from each mouse colon were fixed in 8% neutrally buffered formalin for 20 min and incubated with anti-mouse primary antibodies (such as anti-mouse Fam3D and Muc2 antibodies) followed by a biotinylated anti-Ig secondary antibody (BD Biosciences) and streptavidin-PE or FITC. DAPI was used to stain the nucleus. Viewing fields (4-8 fields) from each slide were captured under fluorescence microscope. The result of each viewing field was quantitated with the NIH ImageJ software.

CT26 mouse epithelial cells were seeded in 35 mm dishes with 14 mm coverslips in the bottom (MatTek Corporation, MA) at 1×10^6 cells/dish and stimulated with the supernatant from *E. coli* O22H8, or exogenous Fam3D for 20 h. Then, the cells were treated with neutral formalin solution for 20 min and washed. The cells were incubated with anti-mouse primary antibodies followed by a biotinylated anti-Ig secondary antibody (BD Biosciences) and streptavidin-PE. Phalloidin was used to stain actin filaments and DAPI was used to stain nuclei.

2.8. Western Immunoblotting

Colon segments 6-cm were ligated at two ends and infused with *E. coli* supernatant (4×10^8 CFU/ml, 300 μl per colon). The colonic mucosae were then scraped and lysed with 1× SDS sample buffer at the indicated timepoints. CT26 cells grown in 60-mm dishes to sub-confluency were cultured for 3 h in FCS-free MDEM. After treatment with exogenous Fam3D, the cells were lysed with 1× SDS sample buffer. All samples were sonicated for 15 s and heated at 100°C for 5 min. The cell lysate was centrifuged at 12,000 rpm (13,523 g) (4°C) for 10 min. The concentration of protein was determined by DC protein Assay from Bio-Rad Laboratories, Inc. (Hercules, CA). The samples were electrophoresed in 10% gradient SDS-PAGE gels, transferred to nitrocellulose membranes, and blocked with 5% skim milk in PBS. After incubation with primary anti-MKP-1 antibody, the blots were incubated with a secondary antibody linked to HRP, and the protein bands were visualized using SuperSignal West Dura, Extended Duration Substrate from Thermo Scientific (Rockford, IL, USA). The membranes were then stripped with Restore Western blot stripping buffer (Thermo Scientific) for detection of total ERK1/2 as control.

2.9. Statistical Analysis

All statistical tests were performed using GraphPad Prism (GraphPad Software, version 9.0). Values are expressed as the mean ± S.E.M. A P value of < 0.05 was considered statistically significant.

2.10. Study Approval

All animal experiment procedures were governed by the US NIH Guide for the Care and Use of Laboratory Animals (National Academies Press, 2011) and all animal study protocols were approved by the Frederick National Laboratory for Cancer Research Animal Care and Use Committee.

3. Results

3.1. Reduced Muc2 Production and Increased Expression of Pro-Inflammatory Cytokines in the Colon Mucosa of Naïve GF Fam3D$^{-/-}$ Mice

Our previous study showed that the colons of naive SPF *Fam3D*$^{-/-}$ mice exhibited crypt hyperplasia with the length of crypts significantly elongated compared with their WT counterparts. Treatment with antibiotics eliminated the difference in colon crypt length between WT and *Fam3D*$^{-/-}$ mice [23]. Therefore, such crypt overgrowth was likely the result of an imbalance of microbiome in the colon of *Fam3D*$^{-/-}$ mice. In GF *Fam3D*$^{-/-}$ mice, such overgrowth of colon crypts visibly disappeared at 2 (Figure 8A) and 8 weeks old (Figure 1A) as compared to GF *Fam3D*$^{+/+}$ mice. The number of Ki67^{+} (a marker of cell proliferation) epithelial cells is similar in the colon crypts between GF *Fam3D*$^{-/-}$ and *Fam3D*$^{+/+}$ mice at 2 (Figure 8B) and 8 weeks old (Figure 1B), indicating that Fam3D is required for controlling the expansion of microorganisms that stimulated the abnormal proliferation of colon epithelial cells. Interestingly, Muc2 significantly reduced in GF *Fam3D*$^{-/-}$ mice as compared to GF *Fam3D*$^{+/+}$ mice at age of 2 weeks (Figure 1C) and 8 weeks (Figure 1D) unlike specific pathogen free (SPF) mice [23]. The expression of IL-1β (Figure 1E) and TNF-α (Figure 1F), two proinflammatory cytokines, was significantly increased in the colon mucosa of GF *Fam3D*$^{-/-}$ mice, which is similar as our previous results in SPF mice [23]. These results suggest that gut microbes influence the regulation of Muc2 production by Fam3D.

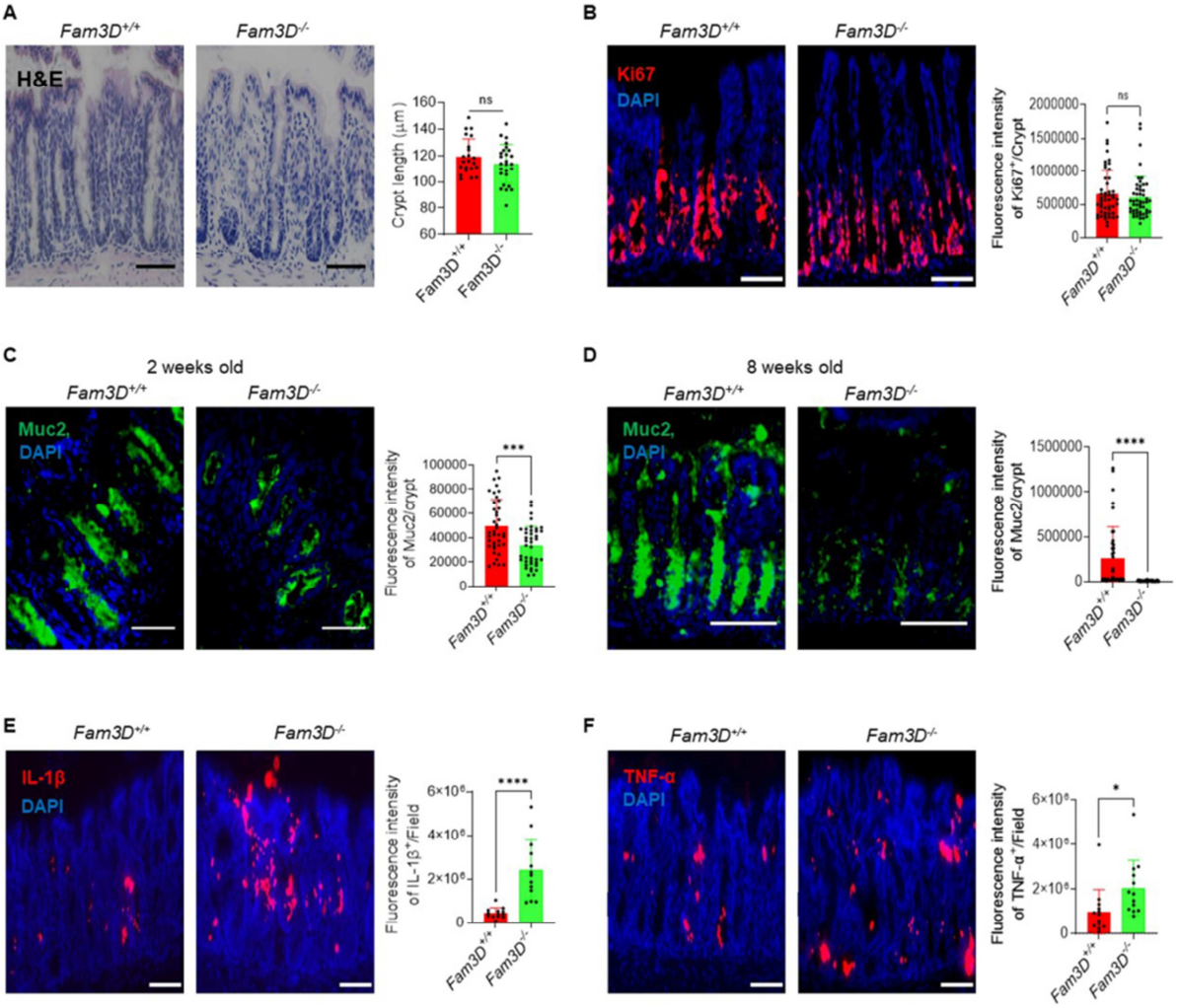

Figure 1. *Reduced Muc2 production and increased expression of pro-inflammatory cytokines in the colon mucosa of naïve GF Fam3D$^{-/-}$ mice.*

A. Similar length of colon crypts between GF *Fam3D*$^{+/+}$ mice and *Fam3D*$^{-/-}$ mice at ages of 8 weeks. H&E staining. Scale bar = 50 μm. Right panel: Quantitation of the length of colon crypts. n = 21-26 crypts from 3 GF mice per group. ns = $P > 0.05$. B. Similar fluorescence intensity of Ki67^{+} cells per crypt at age of 8 weeks. Scale bar = 50 μm. Right panel: Quantitation of fluorescence intensity of Ki67^{+} cells per crypt. n = 49 crypts from 4 GF mice per group. ns = $P > 0.05$. C. Reduced Muc2 production in the colon mucosa of GF *Fam3D*$^{-/-}$ mice at age of 2 weeks. Scale bar = 30 μm. Green: Muc2, Blue: DAPI. Right panel: Quantitation of the fluorescence intensity of Muc2 per crypt. n = 40 crypts from 4 GF mice per group. D. Reduced production of Muc2 in colon mucosa of GF *Fam3D*$^{-/-}$ mice at age of 8 weeks. Scale bar = 30 μm. Green: Muc2, Blue: DAPI. Right panel: Quantitation of the Muc2^{+} fluorescence per crypt. n = 40 crypts from 4 GF mice per group. *** $P < 0.001$. E. Increased IL-1β expression in the colon mucosa of naïve GF *Fam3D*$^{-/-}$ mice. Red: IL-1β, Blue: DAPI. Scale bar = 50 μm. Right panel: Quantitative IL-1β^{+} fluorescence intensity, 13 fields from 4 GF mice per group. ****$P < 0.0001$. F. Increased TNF-α expression in the colon mucosa of naïve GF *Fam3D*$^{-/-}$ mice. Red: IL-1β, Blue: DAPI. Scale bar = 50 μm. Right panel: Quantitative TNF-α^{+} fluorescence intensity, 13 fields from 4 GF mice per group. *$P < 0.05$.

3.2. Increased Susceptibility of GF Fam3D$^{-/-}$ Mice to E. coli Colonization and Development of More Severe Colitis

To examine the susceptibility of GF mice to infection by *E. coli,* GF mice were orally inoculated with *E. coli*. As shown in Figure 2A, Fam3D secreted to the surface of colon mucosa was increased in GF *Fam3D*$^{+/+}$ mice, representing a reaction to challenge by a noxious agent. The diameter of *E. coli* accumulation in the colon lumen (Figure 2B) and the number of *E. coli* in the feces (Figure 2C) were significantly increased in GF *Fam3D*$^{-/-}$ mice. More *E. coli* colonies were found in close contact with or invading into the colon mucosa of GF *Fam3D*$^{-/-}$ mice (Figure 2D), which was associated with increased epithelial cell death (Figure 2E) and severe damage with multiple ulcers (Figure 3F). Muc2 secretion in the colon mucosa was also significantly increased in GF *Fam3D*$^{+/+}$ mice and only small amounts of *E. coli* were found in the outer layer of colonic mucus (Left panel in Figure 2G). In contrast, the secretion of Muc2 was significantly reduced with almost absence of inner layer of mucin and the number of *E. coli* colonizes on the surface of colon mucosa was increased and active invasion into the epithelial cell layer (Right panel in Figure 2G) in GF *Fam3D*$^{-/-}$ mice. These findings indicate that in the absence of colon microbiota, Fam3D deficiency results in reduced Muc2 production allowing more *E. coli* to gain access to the colon epithelial surface.

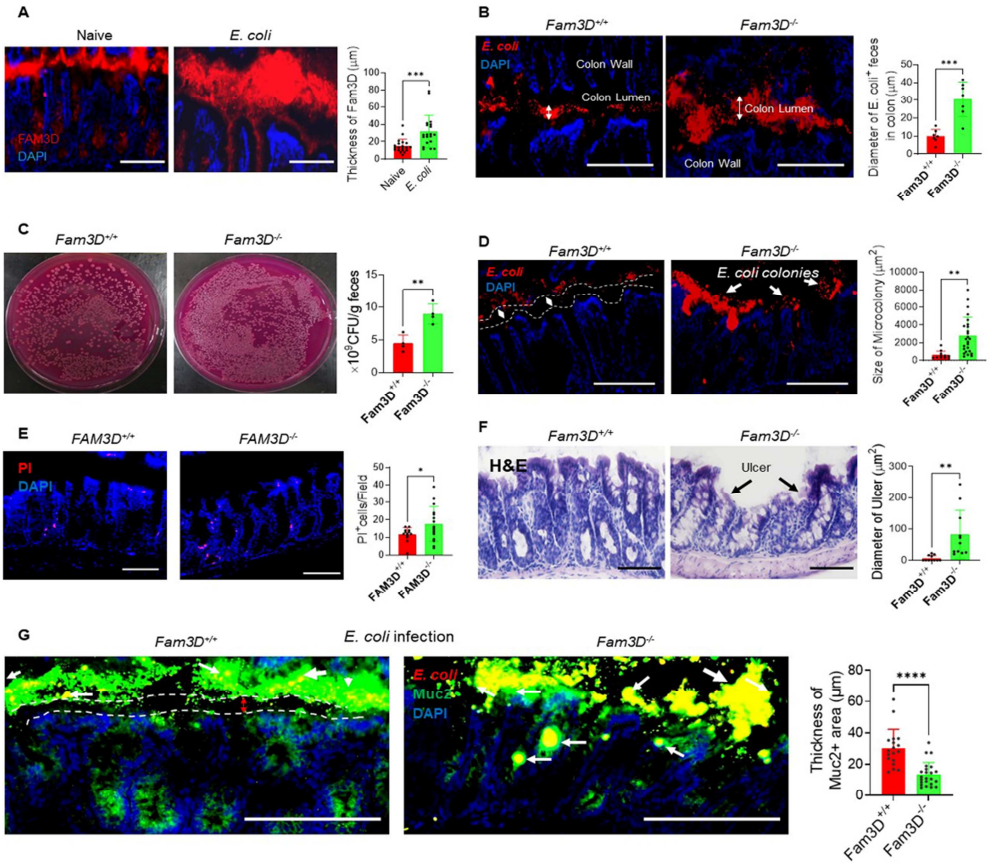

Figure 2. *Increased susceptibility of GF Fam3D$^{-/-}$ mice to E. coli colonization and development of more severe colitis.*

A. *E. coli* infection stimulated Fam3D secretion in the colon mucosa of *Fam3D*$^{+/+}$ GF mice. Red: Fam3D, Blue: DAPI. Scale bar = 100 μm. Right panel: Quantitation of the thickness of Fam3D^{+} secretion on the surface of colon mucosa of GF *Fam3D*$^{+/+}$ mice. ***P< 0.001. n = 20 fields from 3 GF mice per group. B. Higher proliferation of *E. coli* in the colon of GF *Fam3D*$^{-/-}$ mice. Red: *E. coli*, Blue: DAPI. White arrow: *E. coli* in colon lumen. Scale bar =100 μm. Right panel: Quantitation of the diameter for *E. coli*$^{+}$ contents in the colon of GF mice infected with *E. coli*. ***P< 0.001. n = 7 fields from 3 GF mice per group. C. Significantly increased *E. coli* population in the feces of GF *Fam3D*$^{-/-}$ mice. *E. coli* was isolated by Violet red bile lactose (VRBL) agar. Right panel: The results were displayed as CFU (Log10) per g stool from GF mice infected with *E. coli*, n = 4 GF mice per group. **P< 0.01. D. *E. coli* forms more colonies on the colon mucosa of GF *Fam3D*$^{-/-}$ mice. Red: *E. coli* colonies; Blue: DAPI. Dotted lines: Inner layer impermeable to *E. coli*. White arrows: *E. coli* colonies. Scale bar =100 μm. Right panel: Quantitation of the size of *E. coli-forming* colonies in the colon of GF mice infected with *E. coli*. **P< 0.01. n = 11-24 *E. coli* colonies from 3 GF mice per group. E. Increased colon epithelial cell death in GF *Fam3D*$^{-/-}$ mice infected with *E. coli*. Red: PI+ cells, Blue: DAPI. Scale bar = 50 μm. Right panel: Quantitation of PI^{+} cells/field. n = 13-16 fields from 3 GF mice per group. *P < 0.05. F. *E. coli* caused more severe damage to colon mucosa of *Fam3D*$^{-/-}$ mice. H&E staining. Black arrows: Ulcers. Scale bar =100 μm. Right panel: Quantitation of the diameters of ulcers. **P< 0.01. n = 8-11 fields from 4 GF mice per group. G. Fam3D deficiency reduced the protective effect against *E. coli* infection in the colon mucosa. *Fam3D*$^{-/-}$ mice showed absence of inner layer of mucin and increased *E. coli* number and contact to colon mucosa. Red: *E. coli*, Green: Muc2, Blue: DAPI, White arrows: *E. coli*. Dotted lines: Inner layer impermeable to *E. coli*. Scale bar = 100. Right panel: Quantitation of the thickness of Muc2^{+} area on the surface of colon mucosa. ****P< 0.0001. n = 18-23 fields from 3 GF mice per group.

3.3. Increased Susceptibility of GF Fam3D$^{-/-}$ Mice to Chemically Induced Colitis and Carcinogenesis

In SPF mice, Fam3D deficiency markedly increased the severity of inflammation in DSS-induced colitis. All *Fam3D*$^{-/-}$ mice died by day 9 post DSS intake, in contrast to the day 12 shown by *Fam3D*$^{+/+}$ mice. Antibiotics significantly reduced the severity of colitis in *Fam3D*$^{-/-}$ mice [23], suggesting the contribution of dysbiosis to the development of colitis. In GF mice with chemically induced colitis, all *Fam3D*$^{-/-}$ mice died by day 8 post DSS intake, in contrast to the day 10 shown by *Fam3D*$^{+/+}$ mice (Figure 3A). GF *Fam3D*$^{-/-}$ mice also showed more rapid body weight loss as compared with GF *Fam3D*$^{+/+}$ mice (Figure 3B). Pathohistological changes in colon mucosa by day 7 post DSS intake showed more severe damage to the colon crypts in GF *Fam3D*$^{-/-}$ mice (Figure 3C). Muc2 in each crypt was significantly reduced in *Fam3D*$^{-/-}$ mice as compared to *Fam3D*$^{+/+}$ mice (Figure 3D).

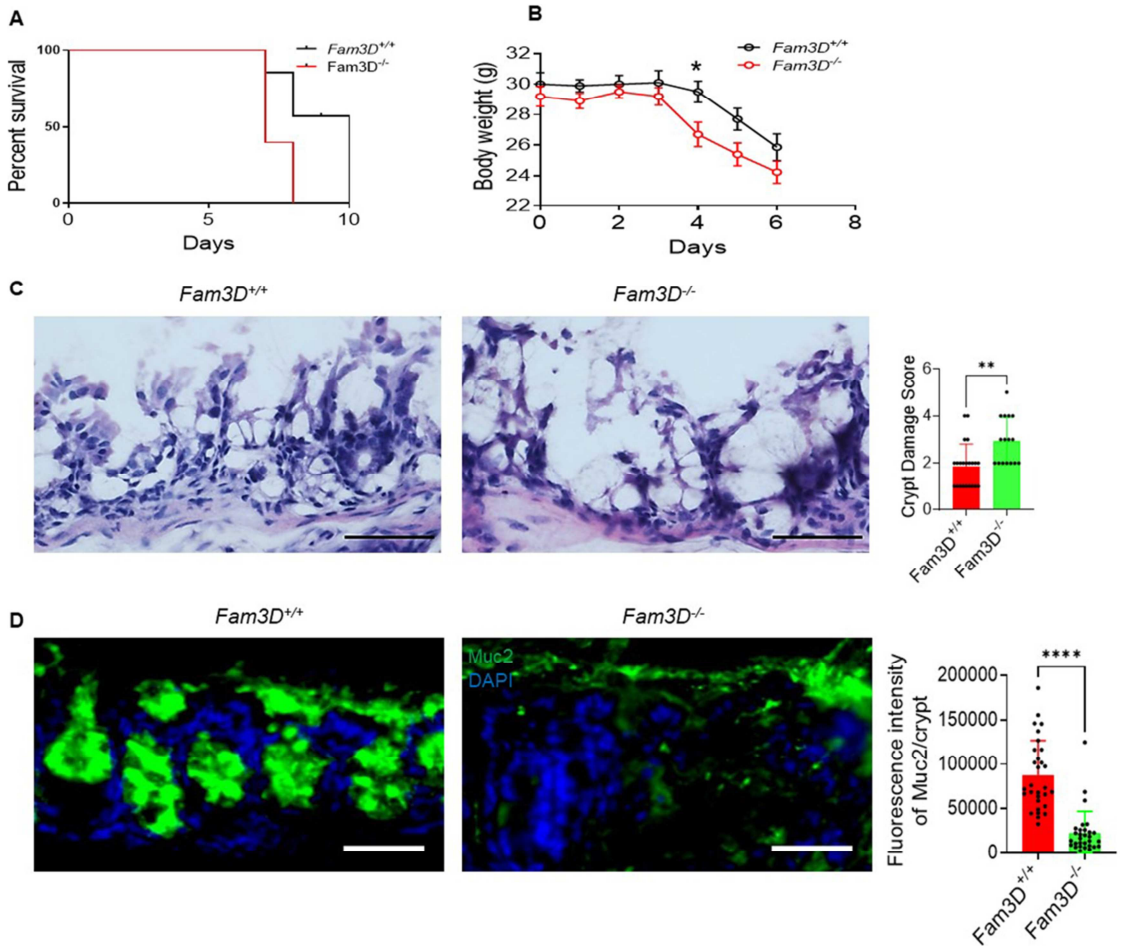

Figure 3. *Increased susceptibility of GF Fam3D$^{-/-}$ mice to chemically induced colitis.*

A. The survival of GF mice. GF *Fam3D*$^{+/+}$ and *Fam3D*$^{-/-}$ mice were given 3.0% DSS in drinking water for 5 days followed with normal water. n = 5 per group. Mouse death was defined by 20% body weight loss and bad status. B. Body weight of GF mice. *Fam3D*$^{+/+}$ and *Fam3D*$^{-/-}$ mice were given 3.0% DSS in drinking water for 5 days followed with normal water. **P* < 0.05. n = 5 per group. C. Distal section of the colons examined by H&E staining. Scale bar = 30 μm. Right panel: Crypt damage scores. n = 16-22 fields from 5 GF mice per group. ***P*< 0.01. D. Reduced Muc2 production in the colon mucosa of *Fam3D*$^{-/-}$ mice with colitis. Green: Muc2, Blue: DAPI. Scale bar = 30 μm. Right panel: Quantitation of the Muc2^{+} fluorescence intensity/crypt. *****P*< 0.0001, n = 30 crypts from 3 GF mice per group.

Since all GF mice died by day 8-10 post DSS intake, these mice were pre-orally inoculated with low levels of *E. coli* [25] which increased the survival of mice with AOM-DSS-induced tumor in both *Fam3D*$^{+/+}$ (7/8) mice and *Fam3D*$^{-/-}$ mice (6/8) (Figure 4A-B). By end of the experiment, the number (Figure 4C) and size (Figure 4D) of tumors were significantly increased in the colon of GF *Fam3D*$^{-/-}$ mice. The characteristic necrotic debris in the glandular lumina termed “dirty necrosis”, was also increased in tumor tissues of GF *Fam3D*$^{-/-}$ mouse colon (Red triangle in Figure 4D), indicating the active growth and invasiveness of the tumors [26]. Muc2 expression was significantly reduced in the mucosa adjacent to tumors of GF *Fam3D*$^{-/-}$ mice (Figure 4E). Interestingly, Muc2 expression was almost undetectable in tumor tissue of both GF *Fam3D*$^{+/+}$ and GF *Fam3D*$^{-/-}$ mice (Figure 4F). These results indicate that Muc2 is crucial for the colonic protection against colon inflammation and cancer.

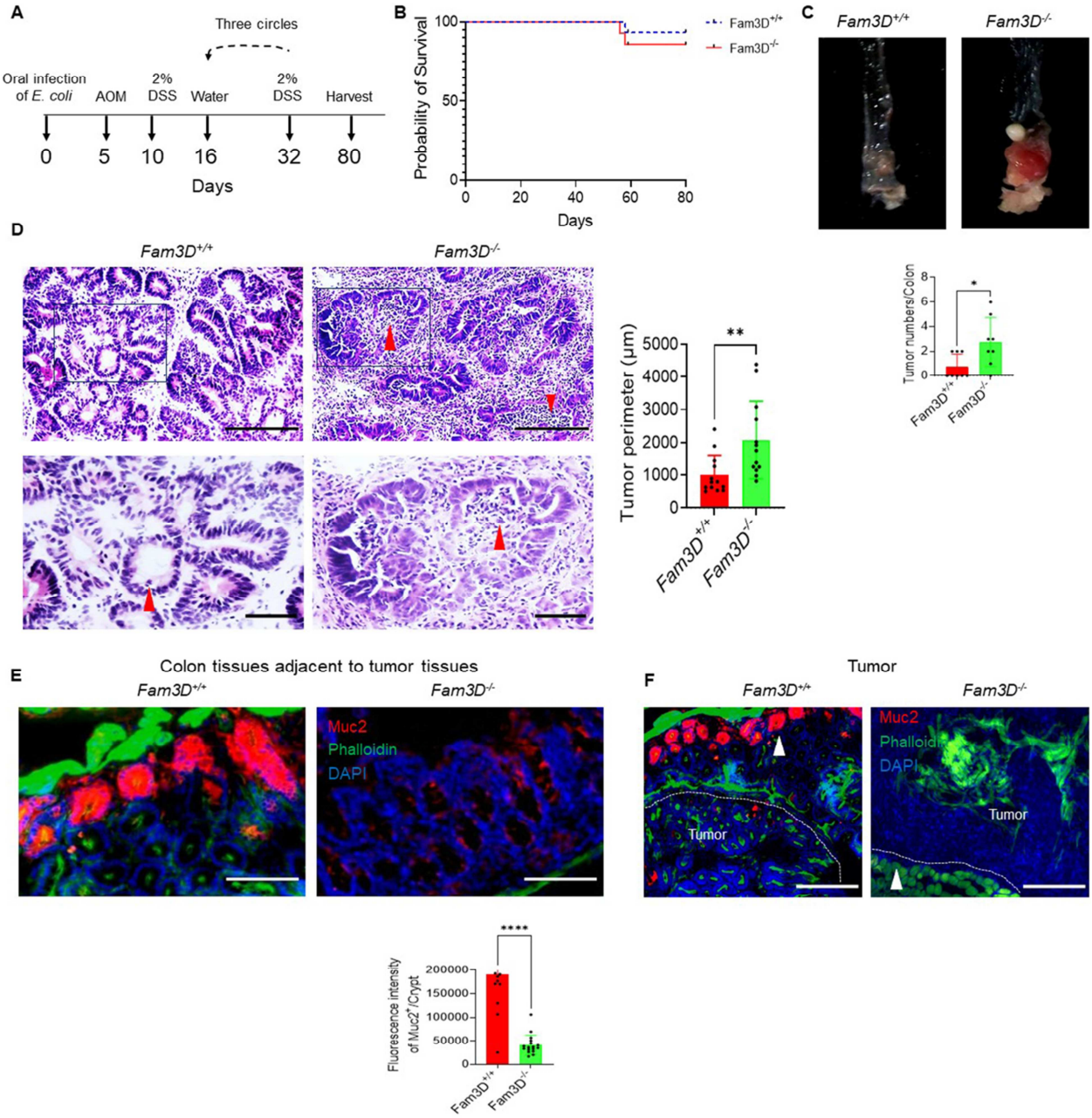

Figure 4. *Increased susceptibility of GF Fam3D$^{-/-}$ mice to AOM-DSS induced colon cancer.*

A. Schematic depicting experimental setup. B. Survival curves of GF mice. C. The number of tumors in the colon of GF *Fam3D*$^{+/+}$ and *Fam3D*$^{-/-}$ mice. Lower panel: Quantitation of the number of tumors in the colon of GF *Fam3D*$^{+/+}$ and *Fam3D*$^{-/-}$ mice. n = 8 GF mice per group. *$P < 0.05$. D. Tumors in the colon examined by H&E staining. Red triangle: Increased characteristic necrotic debris in glandular lumina (so-called "dirty necrosis") in the tumor tissues of the colon of *Fam3D*$^{-/-}$ mice. Upper panel: Scar bar = 100 μm; Lower panel: Scar bar = 30 μm. Right panel: Quantitation of the tumor perimeters in the sections stained by H&E. n = 13 from 6 GF mice per group. **$P < 0.01$. E. Reduced Muc2 expression in colon tissues adjacent to tumor in *Fam3D*$^{-/-}$ mice. Red: Muc2, Green: Phalloidin, Blue: DAPI. Scale bar = 100 μm. Lower panel: Quantitation of the Muc2^{+} fluorescence intensity/crypt. ****$P< 0.0001$. n = 13-17 Crypts from 3 GF mice per group. F. Reduced Muc2 expression in colon tumor tissues of both GF *Fam3D*$^{+/+}$ and *Fam3D*$^{-/-}$ mice. Red: Muc2, Green: Phalloidin, Blue: DAPI. Scale bar = 100 μm. White triangle: Adjacent colon tissues to tumor tissues.

3.4. Increased Inflammatory Responses in the Colon Mucosa of GF Fam3D$^{-/-}$ Mice with Colitis and Colon Cancer

In DSS-induced colitis, GF *Fam3D*$^{-/-}$ mouse colon showed that the production of IL-1β (Figure 5A) and TNF-α (Figure 5B) was significantly increased in the colon mucosa by day 7 post DSS intake. In AOM-DSS-induced colon cancer, the expression of IL-1β (Figure 5C) and TNF-α (Figure 5D) was significantly increased in the colon tissue adjacent to tumors of GF *Fam3D*$^{-/-}$ mice. In tumor tissues, the expression of IL-1β (Figure 5E) and TNF-α (Figure 5F) were also significantly increased in GF *Fam3D*$^{-/-}$ mice. These results suggest that

reduced Muc2 production in the colon mucosa of GF *Fam3D*$^{-/-}$ mice increased inflammatory responses in the colon mucosa.

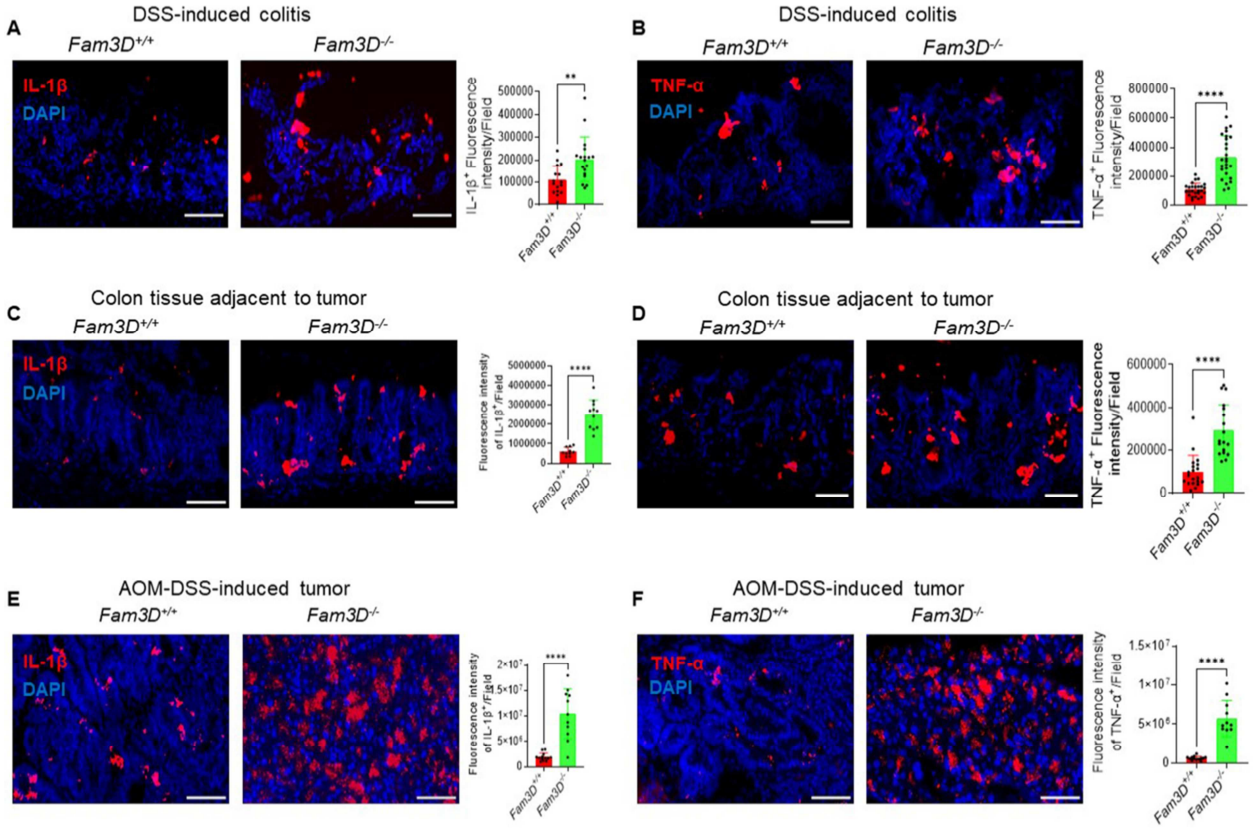

Figure 5. *Increased inflammatory responses in the colon mucosa of GF Fam3D*$^{-/-}$ *mice with colitis and tumor.*

A. Increased IL-1β expression in the colon mucosa of GF *Fam3D*$^{-/-}$ mice with colitis. Red: IL-1β, Blue: DAPI. Scale bar = 50 μm. Right panel: Quantitative IL-1β^{+} fluorescence intensity/field, 16-18 fields from 3 GF mice per group. $^{**}P < 0.01$. B. Increased TNF-α expression in the colon mucosa of GF *Fam3D*$^{-/-}$ mice with colitis. Red: TNF-α, Blue: DAPI. Scale bar = 50 μm. Right panel: Quantitative TNF-α^{+} fluorescence intensity/field, 26 fields from 3 GF mice per group. $^{****}P < 0.0001$. C. Increased IL-1β production in the colon mucosa adjacent to tumor of GF *Fam3D*$^{-/-}$ mice. Red: IL-1β, Blue: DAPI. Scale bar = 50 μm. Right panel: Quantitative IL-1β^{+} fluorescence intensity/field, 13 fields from 4 GF mice per group. $^{****}P < 0.0001$. D. Increased TNF-α production in the colon mucosa adjacent to tumor of GF *Fam3D*$^{-/-}$ mice. Red: TNF-α, Blue: DAPI. Scale bar = 50 μm. Right panel: Quantitative TNF-α^{+} fluorescence intensity/field, 18-20 fields from 4 GF mice per group. $^{****}P < 0.0001$. E. Increased IL-1β expressed in colon tumor tissues of GF *Fam3D*$^{-/-}$ mice. Red: IL-1β, Blue: DAPI. Scale bar = 50 μm. Right panel: Quantitative IL-1β^{+} fluorescence intensity/field, 11-13 fields from 4 GF mice per group. $^{****}P < 0.0001$. F. Increased TNF-α expressed in the colon tumor tissues of GF *Fam3D*$^{-/-}$ mice. Red: TNF-α, Blue: DAPI. Scale bar = 50 μm. Right panel: Quantitative TNF-α^{+} fluorescence intensity/field, 11-13 fields from 4 GF mice per group. $^{****}P < 0.0001$.

3.5. Reduced MKP-1 Production in the Colon Mucosa of GF Fam3D$^{-/-}$ *Mice with E. coli Infection, Colitis, and Cancer*

Since Fam3D deficiency increased pro-inflammatory cytokines in the colon mucosa under naïve, colitis, and cancer, it is necessary to investigate the expression of MKP-1, a negative feedback regulator of MAPK involved in transcription of multiple cytokine genes [19]. After oral inoculation with *E. coli*, MKP-1 expression was significantly increased in the colon mucosa of GF *Fam3D*$^{+/+}$ mice as compared to naïve GF *Fam3D*$^{+/+}$mice (Figure 6A). In contrast, no significant change in MKP-1 expression was detected after *E. coli* infection in GF *Fam3D*$^{-/-}$ mice as compared to naïve GF *Fam3D*$^{-/-}$ mice (Figure 6B). To confirm the effect of *E. coli* on MKP-1 expression, *E. coli* culture supernatant was used to infuse the colon from *Fam3D*$^{+/+}$ and *Fam3D*$^{-/-}$ mice and found that *E. coli* culture supernatant induced MKP-1 expression in the colon mucosa of GF *Fam3D*$^{+/+}$ mice. In contrast, the supernatant failed to induce a rapid MKP-1 expression in the colon mucosa of GF *Fam3D*$^{-/-}$ mice (Figure 6C). In DSS-induced colitis and AOM-DSS-induced colon cancer, MKP-1 expression was also significantly reduced in the colon mucosa of GF *Fam3D*$^{-/-}$ mice with colitis (Figure 6D) and in the colon mucosa adjacent to tumor in GF *Fam3D*$^{-/-}$ mice (Figure 6E). However, MKP-1 expression was almost undetectable in the tumor tissue of both *Fam3D*$^{+/+}$ and *Fam3D*$^{-/-}$ mice (Figure 6F). In vitro, Fam3D induced MKP-1 expression in CT26 mouse colon epithelial cells in a time- and dose dependent manner (Figure 6G-H). These results indicate that increased inflammatory responses resulted from Fam3D deficiency is a causative factor for reduced MKP-1 expression.

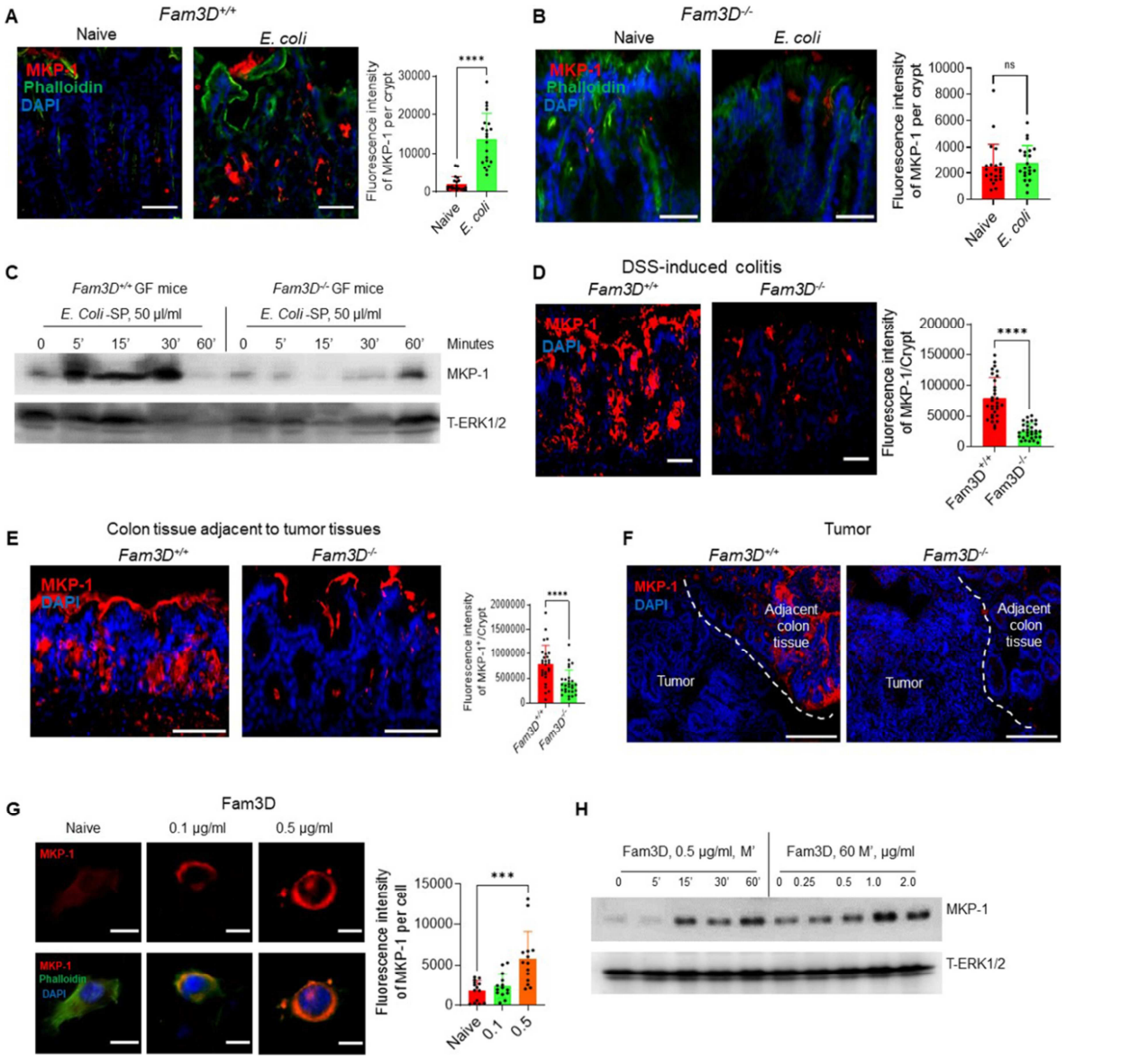

Figure 6. *Reduced MKP-1 production in the colon mucosa of GF Fam3D$^{-/-}$ mice with E. coli infection, colitis, and cancer.*

A-C. *E. coli* infection induced MKP-1 expression. A. Increased MKP-1 expression in the colon mucosa of GF *Fam3D*$^{+/+}$ mice after *E. coli* infection. Red: MKP-1, Green: Phalloidin, Blue: DAPI. Scale bar = 30 μm. Right panel: Quantitation of MKP-1^{+} fluorescence intensity per crypt. ****P< 0.0001. n = 21crypts from 3 GF mice per group. B. *E. coli* infection failed to increase MKP-1 expression in the colon mucosa of GF *Fam3D*$^{-/-}$ mice. Red: MKP-1, Green: Phalloidin, Blue: DAPI. Scale bar = 30 μm. Right panel: Quantitation of MKP-1^{+} fluorescence intensity per crypt. *ns*= P> 0.05. n = 22 crypts from 3 GF mice per group. C. Western immunoblotting showed reduced production of MKP-1 protein in *Fam3D*$^{-/-}$ colon mucosa after stimulation of *E. coli* supernatant. Left part: MKP-1 production in the colon mucosa of GF *Fam3D*$^{+/+}$ mice. Right part: MKP-1 production in the colon mucosa of GF *Fam3D*$^{-/-}$ mice. D. Reduced MKP-1 expression in the colon mucosa of *Fam3D*$^{-/-}$ mice with colitis. Red: MKP-1, Blue: DAPI. Scale bar = 30 μm. Right panel: Quantitation of the MKP-1^{+} fluorescence intensity per crypt. ****P< 0.0001. n = 30 crypts from 4 GF mice per group. E. Reduced MKP-1 expression in colon tissues adjacent to tumor in *Fam3D*$^{-/-}$ mice. Red: MKP-1, Blue: DAPI. Scale bar = 50 μm. Right panel: Quantitation of the MKP-1^{+} fluorescence intensity per crypt. ****P< 0.0001. n = 28 crypts from 4 GF mice per group. F. Reduced MKP-1 expression in the colon tumor tissues of both GF *Fam3D*$^{+/+}$ and *Fam3D*$^{-/-}$ mice. Red: MKP-1, Blue: DAPI. Scale bar = 100 μm. G. Exogenous Fam3D induced MKP-1 expression in CT26 mouse colon epithelial cells. Scale bar = 10 μm. Red: MKP-1, Green: Phalloidin, Blue: DAPI. Right panel: Quantitation of the MKP-1^{+} fluorescence intensity per cell. ***P< 0.001. n = 14 cells per group. H. Fam3D induced MKP-1 expression in CT26 cells was detected by Wester blotting. Left part: Fam3D-induced MKP-1 expression is time-dependent; Right part: Fam3D-induced MKP-1 expression is dose-dependent.

3.6. Fpr1 and Fpr2 Were Required for Fam3D to Induce Muc2 Upregulation

In vitro, the supernatant from *E. coli* increased Fam3D production in CT26 mouse colon epithelial cells (Figure 9A). Since lipopolysaccharide (LPS) as the major outer membrane component of *E. coli*, LPS was used to stimulate CT26 cells. As shown in Figure 7A, LPS induced production of Fam3D. The TLR4 inhibitor can attenuate LPS-induced Fam3D production (Figure 7B). These results indicate that *E. coli* (LPS) interacted with TLR4 to promote Fam3D production in colon epithelial cells.

Further study showed that exogenous Fam3D can induce the production of Muc2 (Figure 7C). Both Fpr1 and Fpr2 were required for Fam3D to activate CT26 cells because fMLF (an agonist for both Fpr1 and Fpr2), MMK-1 (an agonist for Fpr2) and recombinant Fam3D induced CT26 cell chemotaxis (Figure 9B), which was partially attenuated by CsH (an antagonist for Fpr1) (Figure 9C) or WRW4 (an antagonist for Fpr2) (Figure 9D). CsH combined with WRW4 completely inhibited Fam3D-induced CT26 cell chemotaxis (Figure 9E). On the other hand, bone marrow neutrophils isolated from WT, *Fpr1*$^{-/-}$, *Fpr2*$^{-/-}$ and double *Fpr1/2*$^{-/-}$ mice were also used to confirm the receptor usage by Fam3D. As shown in Figure 9F-I, *Fpr1*$^{-/-}$ or *Fpr2*$^{-/-}$ bone marrow neutrophils exhibited partial reduction in chemotactic response to Fam3D. However, double *Fpr1/2*$^{-/-}$ neutrophils completely lost migratory response to Fam3D. Exogenous Fam3D induced Muc2 production in CT26 cells, which can be significantly reduced By Boc-MLF (an antagonist for Fpr1) or WRW4. Boc-MLF combined with WRW4 completely inhibited Fam3D-induced Muc2 production in CT26 cells (Figure 7D). These results indicate that *E. coli* supernatant stimulates Fam3D production by TLR4 and Fpr1 and Fpr2 are required for Fam3D to induce Muc2 production in colon epithelial cells.

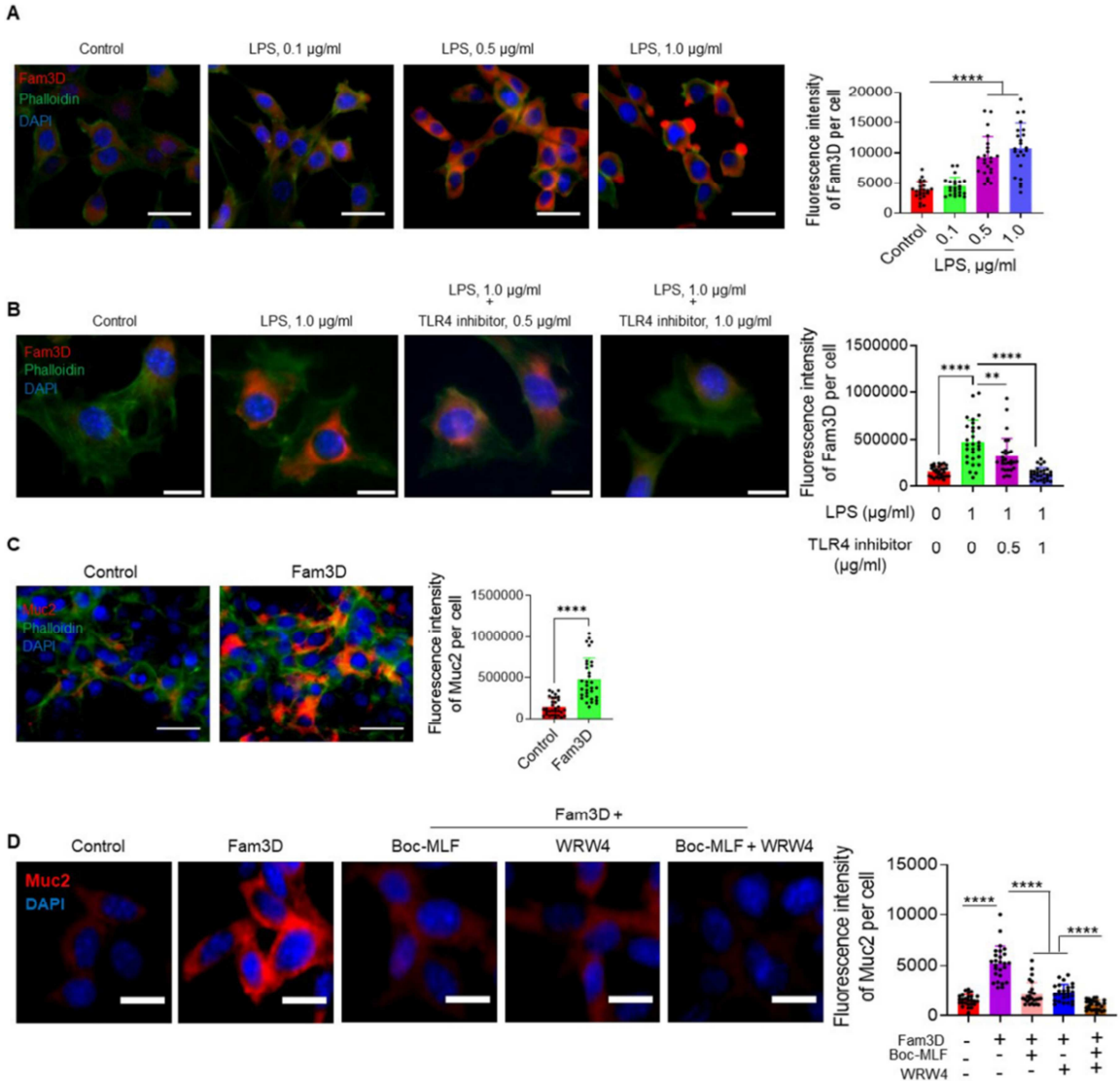

Figure 7. *Fpr1 and Fpr2 were required for Fam3D to induce Muc2 upregulation.*

A. LPS induced Fam3D expression in CT26 cells in a dose-dependent manner. Red: Fam3D, Green: Phalloidin, Blue: DAPI. Scale bar = 20 μm. Right panel: Quantitation of the Fam3D+ fluorescence intensity per cell. ****P< 0.0001. n = 23 cells per group. B. LPS-induced Fam3D expression was attenuated by TLR4 inhibitor. Red: Fam3D, Green: Phalloidin, Blue: DAPI. Scale bar = 5 μm. Right panel: Quantitation of Fam3D+ fluorescence intensity per cell. n = 29 cells per group. **P < 0.01, **** P < 0.0001. C. Fam3D induced Muc2 expression in CT26 cells. Red: Muc2, Green: Phalloidin, Blue: DAPI. Scale bar = 10 μm. Right panel: Quantitation of Muc2+ fluorescence intensity per cell. n = 32 cells per group. **** P < 0.0001. D. Fam3D-induced Muc2 production was attenuated by Fpr1 and Fpr2 inhibitors. Boc-MLP: Fpr1 antagonist, WRW4: Fpr2 antagonist. Red: Muc2, Blue: DAPI. Scale bar = 10 μm. Right panel: Quantitation of Muc2+ fluorescence intensity per cell. n = 26 cells per group. **** P < 0.0001.

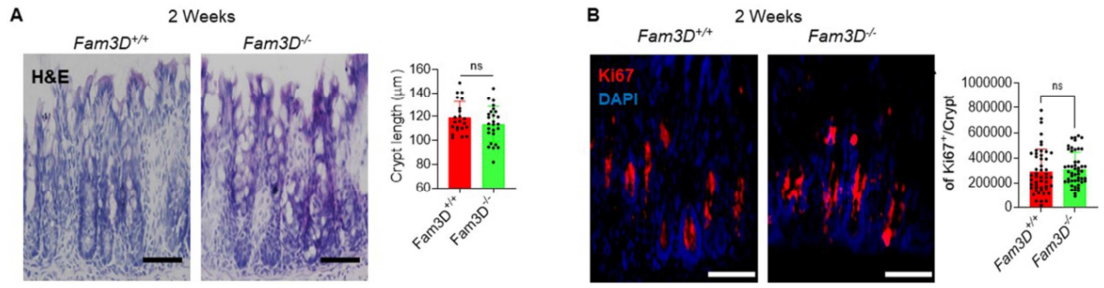

Figure 8. *Similar colon crypt length and Ki67 $^{+}$ cells between GF Fam3D$^{-/-}$ and Fam3D$^{+/+}$ mice at 2 weeks old.*

A. Similar length of colon crypts between GF *Fam3D*$^{+/+}$ mice and *Fam3D*$^{-/-}$ mice at age of 2 weeks. H&E staining. Scale bar = 50 μm. Right panel: Quantitation of the length of colon crypts. n = 21-26 crypts from 3 GF mice per group. ns = $P > 0.05$. B. Similar fluoresceine intensity of Ki67^{+} cells per crypt at age of 2 weeks. Scale bar = 50 μm. Right panel: Quantitation of fluorescence intensity of Ki67^{+} cells per Crypt. n = 49 crypts from 3 GF mice per group. ns = $P > 0.05$.

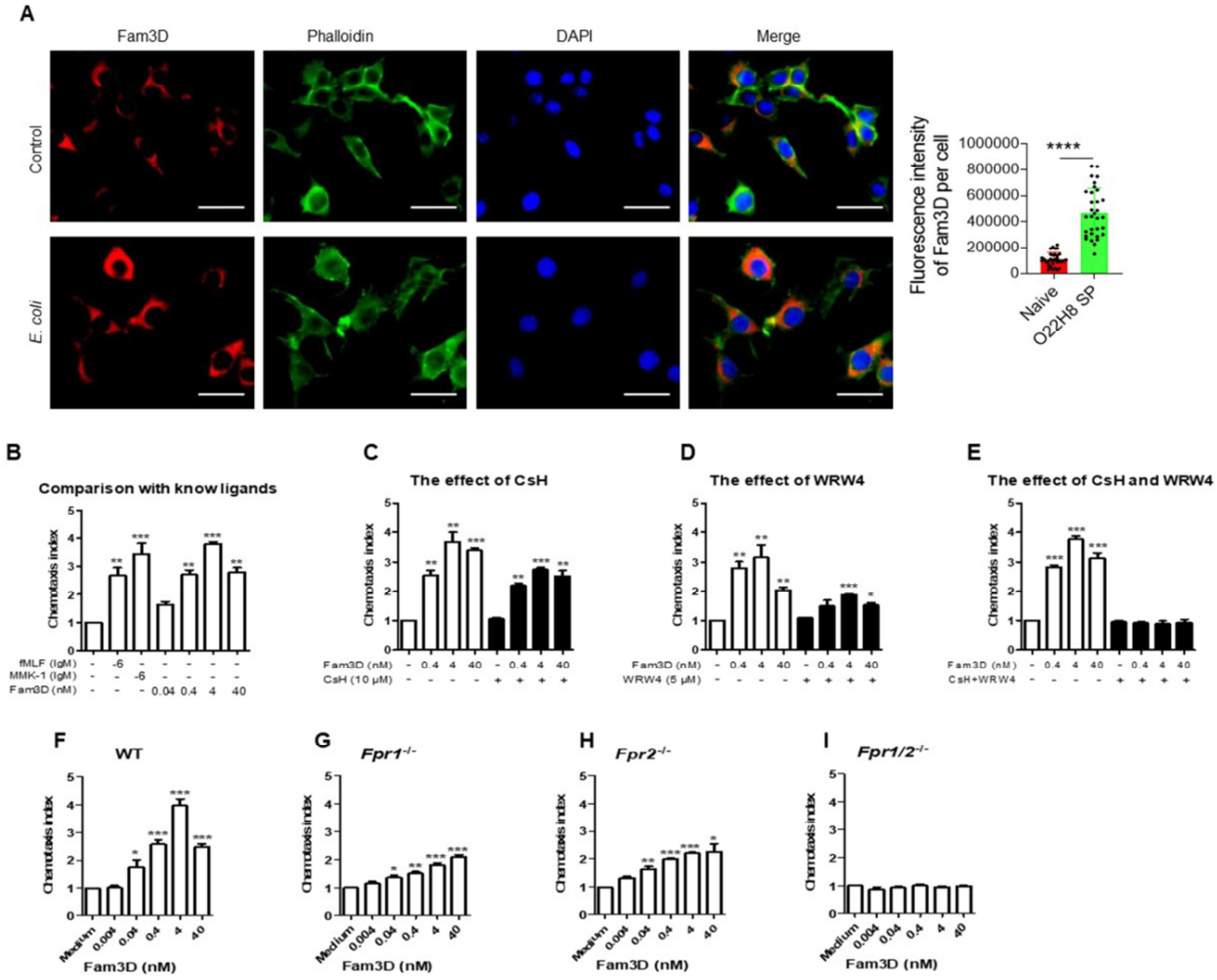

Figure 9. *Increased Fam3D expression by E. coli supernatant in CT26 cells and Fam3D mediates CT26 cell migration through Fpr1 and Fpr2.*

A. *E. coli* supernatant induced Fam3D expression by CT26 cells. Red: Fam3D, Green: Phalloidin, Blue: DAPI. Scale bar = 20 μm. Right panel: Quantitation of Fam3D^{+} fluorescence intensity per cell. ****P< 0.0001. n = 32 cells per group. B-I. Chemotaxis assays for CT26 cells and neutrophils. Cells were performed with 48-well chemotaxis chambers and polycarbonate filters (8-μm or 5-μm pore size) (NeuroProbe, Cabin John, MD). The results are expressed as the mean ± S.D. of the chemotaxis index, which represents the fold increase in the number of migrated cells, counted in three high power fields (×400), in response to chemoattractants over spontaneous cell migration (to control medium). B-E. Fam3D-induced CT26 cell chemotaxis was completely inhibited by blockage of Fpr1 and Fpr2. B. fMLF, MMK-1 and Fam3D induced CT26 cell chemotaxis. C. CsH, an antagonist for Fpr1, partly inhibited Fam3D-induced CT26 cell chemotaxis. D. WRW4, an antagonist for Fpr2, partly inhibited Fam3D-induced CT26 cell chemotaxis. E. CsH combined with WRW4 completely inhibited Fam3D- induced CT26 cell chemotaxis. **$P < 0.01$, ***$P < 0.001$. F-I. Fam3D-induced bone marrow neutrophil chemotaxis was completely inhibited by absence of Fpr1 and Fpr2. F. Fam3D induced chemotaxis of neutrophils from the bone marrow of WT mice. G. Fam3D induced chemotaxis was partly inhibited in the neutrophils from the bone marrow of *Fpr1*$^{-/-}$ mice. H. Fam3D induced chemotaxis was partly inhibited in the neutrophils from the bone marrow of *Fpr2*$^{-/-}$ mice. I. Fam3D induced chemotaxis was completely inhibited in the neutrophils from the bone marrow of double *Fpr1/2*$^{-/-}$ mice. *$P < 0.05$, **$P < 0.01$, ***$P < 0.001$.

4. Discussion

Mucins are critical in maintaining mucosal homeostasis and protecting the colon mucosa from direct contact between microorganisms, including commensals and pathogens, and colon mucosa. The mucus barrier is formed predominantly by Muc2, a prominent secretory mucin that overlies the intestinal epithelium [27, 28]. Bacterial infection such as *Salmonella* infection led to the increases in luminal Muc2 secretion in WT mice. But *Muc2*$^{-/-}$ mice showed marked susceptibility to *Salmonella* infection, carrying significantly higher cecal and liver pathogen burdens, and significantly developing disruption of barrier and higher mortality rates [28]. *Muc2*$^{-/-}$ mice inoculated with *Citrobacter rodentium* exhibited weight loss and increased *C. rodentium* burdens in stool and bacterial contact to the colonic mucosa and more ulceration in the colon amid focal bacterial microcolonies with higher mortality [7]. In this study, *Fam3D*$^{-/-}$ mice inoculated with *E. coli* displayed reduced Muc2 production, thereby more *E. coli* colonization and increased close contact with colon mucosa, resulting in more epithelial cell death.

MUC2 also plays a significant role in the pathogenesis of IBD, and its deficiency changes the composition of the mucus, exacerbating inflammatory responses [29]. Ulcerative colitis (UC) is an IBD characterized by continuous inflammation of the inner layer of the colon, and the immune responses of the host to microbiome increases after exposure to bacteria [29, 30]. In patients with UC, MUC2 was thinner, and its distribution was more discontinuous. Patients with UC also exhibited reduced number of goblet cells and MUC2 secretion, especially at the onset of severe disease, which enables direct interaction between the epithelial barrier and the colonic microbiota [29, 31-33]. Analysis of the relationship between MUC2 and ulcerative colitis showed that MUC2 mRNA expression levels were unaffected during UC development, but MUC2 protein production was decreased in active UC, indicating the quantity of MUC2 is regulated at the translational level [29, 30]. In mouse model of DSS-induced colitis, *Muc2*$^{-/-}$ mice showed loss of body weight, diarrhea, occult blood loss or gross bleeding. Patients with colorectal adenocarcinoma showed decreased MUC2 expression but preserved in mucinous carcinoma [34, 35]. The loss of MUC2 expression is a poor prognostic factor in the patients with stage II and III colorectal carcinoma [36] and is associated with progression and metastasis in CRC [34, 37, 38]. *Muc2*$^{-/-}$ mice displayed aberrant intestinal crypt morphology and abnormal cell maturation and motility. Most notably, such mice frequently developed adenomas in the small intestine and colorectum that progressed to invasive adenocarcinoma [39]. Furthermore, Muc2 silencing promotes colon cancer metastasis [40]. Thus, Muc2 is involved in the suppression of colorectal cancer development and metastasis [39, 41]. In this study, *E. coli* products such as LPS stimulated Fam3D expression via TLR4 in colon epithelial cells, while Fam3D induced Muc2 production through Fpr1 and Fpr2. Fam3D deficiency reduced Muc2 production.

Inflammatory responses such as increased expression of TNF-α and IL-1β are characteristics of *Muc2*$^{-/-}$ mice [42]. MKP-1 acts as an inducible negative regulator of p38 and JNK MAPKs and serves to restrict the production of pro-inflammatory cytokines [43]. Upon LPS challenge, the activation of p38 and c-Jun NH2-terminal kinase were prolonged and the production of TNF-α and interleukin (IL)-6 were increased in *Mkp-1*$^{-/-}$ cells and *Mkp-1*$^{-/-}$ mice challenged with LPS produced more TNF-α, IL-6, and IL-10 and exhibited a remarkable increase in the mortality [44]. After challenge with peptidoglycan, lipoteichoic acid, and live or heat-killed *Staphylococcus aureus*, *Mkp-1*$^{-/-}$ mice mounted a more robust production of cytokines and chemokines, including TNF-α, IL-6, and IL-10 [45]. Thus, MKP-1 plays a critical role in limiting inflammatory responses to Gram-positive and -negative bacterial infection. MKP-1 is also crucial in the pathogenesis of IBD. In patients with UC or Crohn's disease as well as in WT mice with colitis induced by DSS, the expression of MKP-1 was increased [46]. *Mkp-1*$^{-/-}$ mice were more susceptible to chemically induced colitis and showed more severe crypt injury and inflammation [46]. In colon tumorigenesis, the inflammatory microenvironment surrounding tumors is a critical component that drives tumor progression [47]. IL-1β is an important mediator of cancer-related inflammation and is secreted by immune, stromal and tumor cells [48]. Increased IL-1β levels in colon cancer is associated with more rapid tumor growth and invasion [47]. TNF-α is predominantly produced by macrophages as well as tumor cells. Elevated TNF-α expression in colon cancer tissues also promotes tumor growth, invasion, and metastasis [49]. *Mkp-1 deficiency* promotes tumorigenesis in the mouse model of chemically induced colitis-associated colon cancer [50]. In this study, exogeneous Fam3D increased MKP-1 expression in CT26 mouse colon epithelial cells and GF *Fam3D*$^{-/-}$ mice showed reduced MKP-1 expression and increased IL-1β and TNF-α production.

5. Conclusions

GF *Fam3D*$^{-/-}$ mice showed reduced Muc2 production and MKP-1 expression in colon mucosa under the status of naïve, *E. coli* infection, chemically induced colitis, and colon cancer, thereby increasing *E. coli* colonization and inflammatory responses in the colon mucosa. Thus, Fam3D was demonsreated to be truly a homeostatic protein to limit bacterial proliferation and prevent pathogens from direct contact with the colon mucosa and control the production of pre-inflammatory cytokines and inflammation in colon mucosa. Meanwhile, this study also demonstrated that GF mice are a suitable model to investigate the contribution of microbiome and the precise function of Fam3D in maintaining colon homeostasis under sterile condition.

Author Contributions

KC, Methodology, investigation and writing and revising the manuscript, WL, TY, Participate in the project process, WG, Preparation of experimental materials, SD, GJ, JY, GF mouse experiments, GT, Intellectual inputting, YW and JMW, Supervision of the project.

Conflict of Interest

The authors declare no conflicts of interest with the contents of this article. All authors approved the submitted version.

Data Availability

All data generated or analyzed during this study are included in this manuscript. Further inquiries can be directed to the corresponding authors.

Acknowledgements

We are grateful to Mr. Matthew McCollum and Ms Misty Peck for preparation of samples. We also gratefully acknowledge Ms. Cheri A. Rhoderick for providing secretarial assistance. This project was funded in whole or in part with federal funds from the National Cancer Institute, National Institutes of Health, under Contract No. HHSN261201500003I. The content of this publication does not necessarily reflect the views or policies of the Department of Health and Human Services, nor does mention of trade names, commercial products, or organizations imply endorsement by the U.S. Government. This project was supported in part by the Intramural Research Program of the CIL, CCR, NCI.

References

[1] Terzic J, Grivennikov S, Karin E, *et al.* Inflammation and colon cancer. *Gastroenterology* 2010; 138: 2101-2114 e2105.

[2] Schreuders EH, Ruco A, Rabeneck L, *et al.* Colorectal cancer screening: a global overview of existing programmes. *Gut* 2015; 64: 1637-1649.

[3] Tuomisto AE, Makinen MJ, Vayrynen JP. Systemic inflammation in colorectal cancer: Underlying factors, effects, and prognostic significance. *World J Gastroenterol* 2019; 25: 4383-4404.

[4] Gundamaraju R, Chong WC. Consequence of distinctive expression of MUC2 in colorectal cancers: How much is actually bad? *Biochim Biophys Acta Rev Cancer* 2021; 1876: 188579.

[5] Johansson ME, Ambort D, Pelaseyed T, *et al.* Composition and functional role of the mucus layers in the intestine. *Cell Mol Life Sci* 2011; 68: 3635-3641.

[6] Johansson ME, Phillipson M, Petersson J, *et al.* The inner of the two Muc2 mucin-dependent mucus layers in colon is devoid of bacteria. *Proc Natl Acad Sci U S A* 2008; 105: 15064-15069.

[7] Bergstrom KS, Kissoon-Singh V, Gibson DL, *et al.* Muc2 protects against lethal infectious colitis by disassociating pathogenic and commensal bacteria from the colonic mucosa. *PLoS Pathog* 2010; 6: e1000902.

[8] Liu Y, Yu X, Zhao J, *et al.* The role of MUC2 mucin in intestinal homeostasis and the impact of dietary components on MUC2 expression. *Int J Biol Macromol* 2020; 164: 884-891.

[9] Tadesse S, Corner G, Dhima E, *et al.* MUC2 mucin deficiency alters inflammatory and metabolic pathways in the mouse intestinal mucosa. *Oncotarget* 2017; 8: 71456-71470.

[10] Bu XD, Li N, Tian XQ, *et al.* Altered expression of MUC2 and MUC5AC in progression of colorectal carcinoma. *World J Gastroenterol* 2010; 16: 4089-4094.

[11] Al-Khayal K, Abdulla M, Al-Obaid O, *et al.* Differential expression of mucins in Middle Eastern patients with colorectal cancer. *Oncol Lett* 2016; 12: 393-400.

[12] Johansson ME, Jakobsson HE, Holmen-Larsson J, *et al.* Normalization of Host Intestinal Mucus Layers Requires Long-Term Microbial Colonization. *Cell Host Microbe* 2015; 18: 582-592.

[13] Petersson J, Schreiber O, Hansson GC, *et al.* Importance and regulation of the colonic mucus barrier in a mouse model of colitis. *Am J Physiol Gastrointest Liver Physiol* 2011; 300: G327-333.

[14] Arike L, Holmen-Larsson J, Hansson GC. Intestinal Muc2 mucin O-glycosylation is affected by microbiota and regulated by differential expression of glycosyltranferases. *Glycobiology* 2017; 27: 318-328.

[15] Yao D, Dai W, Dong M, *et al.* MUC2 and related bacterial factors: Therapeutic targets for ulcerative colitis. *EBioMedicine* 2021; 74: 103751.

[16] Zhang W, Liu HT. MAPK signal pathways in the regulation of cell proliferation in mammalian cells. *Cell Res* 2002; 12: 9-18.

[17] Broom OJ, Widjaya B, Troelsen J, *et al.* Mitogen activated protein kinases: a role in inflammatory bowel disease? *Clin Exp Immunol* 2009; 158: 272-280.

[18] Haagenson KK, Wu GS. The role of MAP kinases and MAP kinase phosphatase-1 in resistance to breast cancer treatment. *Cancer Metastasis Rev* 2010; 29: 143-149.

[19] Korhonen R, Moilanen E. Mitogen-activated protein kinase phosphatase 1 as an inflammatory factor and drug target. *Basic Clin Pharmacol Toxicol* 2014; 114: 24-36.

[20] Zhu Y, Xu G, Patel A, *et al.* Cloning, expression, and initial characterization of a novel cytokine-like gene family. *Genomics* 2002; 80: 144-150.

[21] Peng X, Xu E, Liang W, *et al.* Identification of FAM3D as a new endogenous chemotaxis agonist for the formyl peptide receptors. *J Cell Sci* 2016; 129: 1831-1842.

[22] He L, Fu Y, Deng J, *et al.* Deficiency of FAM3D (Family With Sequence Similarity 3, Member D), A Novel Chemokine, Attenuates Neutrophil Recruitment and Ameliorates Abdominal Aortic Aneurysm Development. *Arterioscler Thromb Vasc Biol* 2018; 38: 1616-1631.

[23] Liang W, Peng X, Li Q, *et al.* FAM3D is essential for colon homeostasis and host defense against inflammation associated carcinogenesis. *Nat Commun* 2020; 11: 5912.

[24] Chen K, Yoshimura T, Gong W, *et al.* Requirement of CRAMP for mouse macrophages to eliminate phagocytosed E. coli through an autophagy pathway. *J Cell Sci* 2021; 134.

[25] Lu J, Dong B, Chen A, *et al.* Escherichia coli promotes DSSinduced murine colitis recovery through activation of the TLR4/NFkappaB signaling pathway. *Mol Med Rep* 2019; 19: 2021-2028.

[26] Fleming M, Ravula S, Tatishchev SF, *et al.* Colorectal carcinoma: Pathologic aspects. *J Gastrointest Oncol* 2012; 3: 153-173.

[27] Dharmani P, Srivastava V, Kissoon-Singh V, *et al.* Role of intestinal mucins in innate host defense mechanisms against pathogens. *J Innate Immun* 2009; 1: 123-135.

[28] Zarepour M, Bhullar K, Montero M, *et al.* The mucin Muc2 limits pathogen burdens and epithelial barrier dysfunction during Salmonella enterica serovar Typhimurium colitis. *Infect Immun* 2013; 81: 3672-3683.

[29] Kang Y, Park H, Choe BH, *et al.* The Role and Function of Mucins and Its Relationship to Inflammatory Bowel Disease. *Front Med (Lausanne)* 2022; 9: 848344.

[30] Bankole E, Read E, Curtis MA, *et al.* The Relationship between Mucins and Ulcerative Colitis: A Systematic Review. *J Clin Med* 2021; 10.

[31] Grootjans J, Hundscheid IH, Lenaerts K, *et al.* Ischaemia-induced mucus barrier loss and bacterial penetration are rapidly counteracted by increased goblet cell secretory activity in human and rat colon. *Gut* 2013; 62: 250-258.

[32] Gustafsson JK, Navabi N, Rodriguez-Pineiro AM, *et al.* Dynamic changes in mucus thickness and ion secretion during Citrobacter rodentium infection and clearance. *PLoS One* 2013; 8: e84430.

[33] Sun J, Shen X, Li Y, *et al.* Therapeutic Potential to Modify the Mucus Barrier in Inflammatory Bowel Disease. *Nutrients* 2016; 8.

[34] Blank M, Klussmann E, Kruger-Krasagakes S, *et al.* Expression of MUC2-mucin in colorectal adenomas and carcinomas of different histological types. *Int J Cancer* 1994; 59: 301-306.

[35] Byrd JC, Bresalier RS. Mucins and mucin binding proteins in colorectal cancer. *Cancer Metastasis Rev* 2004; 23: 77-99.

[36] Kang H, Min BS, Lee KY, *et al.* Loss of E-cadherin and MUC2 expressions correlated with poor survival in patients with stages II and III colorectal carcinoma. *Ann Surg Oncol* 2011; 18: 711-719.

[37] Ajioka Y, Allison LJ, Jass JR. Significance of MUC1 and MUC2 mucin expression in colorectal cancer. *J Clin Pathol* 1996; 49: 560-564.

[38] Bresalier RS, Niv Y, Byrd JC, *et al.* Mucin production by human colonic carcinoma cells correlates with their metastatic potential in animal models of colon cancer metastasis. *J Clin Invest* 1991; 87: 1037-1045.

[39] Velcich A, Yang W, Heyer J, *et al.* Colorectal cancer in mice genetically deficient in the mucin Muc2. *Science* 2002; 295: 1726-1729.

[40] Hsu HP, Lai MD, Lee JC, *et al.* Mucin 2 silencing promotes colon cancer metastasis through interleukin-6 signaling. *Sci Rep* 2017; 7: 5823.

[41] Kawashima H. Roles of the gel-forming MUC2 mucin and its O-glycosylation in the protection against colitis and colorectal cancer. *Biol Pharm Bull* 2012; 35: 1637-1641.

[42] Van der Sluis M, De Koning BA, De Bruijn AC, *et al.* Muc2-deficient mice spontaneously develop colitis, indicating that MUC2 is critical for colonic protection. *Gastroenterology* 2006; 131: 117-129.

[43] Li J, Wang X, Ackerman WEt, *et al.* Dysregulation of Lipid Metabolism in Mkp-1 Deficient Mice during Gram-Negative Sepsis. *Int J Mol Sci* 2018; 19.

[44] Zhao Q, Wang X, Nelin LD, *et al.* MAP kinase phosphatase 1 controls innate immune responses and suppresses endotoxic shock. *J Exp Med* 2006; 203: 131-140.

[45] Wang X, Meng X, Kuhlman JR, *et al.* Knockout of Mkp-1 enhances the host inflammatory responses to gram-positive bacteria. *J Immunol* 2007; 178: 5312-5320.

[46] Li J, Wang H, Zheng Z, *et al.* Mkp-1 cross-talks with Nrf2/Ho-1 pathway protecting against intestinal inflammation. *Free Radic Biol Med* 2018; 124: 541-549.

[47] Li Y, Wang L, Pappan L, *et al.* IL-1beta promotes stemness and invasiveness of colon cancer cells through Zeb1 activation. *Mol Cancer* 2012; 11: 87.

[48] Germano G, Allavena P, Mantovani A. Cytokines as a key component of cancer-related inflammation. *Cytokine* 2008; 43: 374-379.

[49] Al Obeed OA, Alkhayal KA, Al Sheikh A, *et al.* Increased expression of tumor necrosis factor-alpha is associated with advanced colorectal cancer stages. *World J Gastroenterol* 2014; 20: 18390-18396.

[50] Hammad A, Zheng ZH, Namani A, *et al.* Transcriptome analysis of potential candidate genes and molecular pathways in colitis-associated colorectal cancer of Mkp-1-deficient mice. *BMC Cancer* 2021; 21: 607.